

AutoGraphAD: A novel approach using Variational Graph Autoencoders for anomalous network flow detection

1st Georgios Anyfantis

*Department of Computer Architecture
Universitat Politècnica de Catalunya
Barcelona, Spain
georgios.anyfantis@upc.edu*

2nd Pere Barlet-Ros

*Department of Computer Architecture
Universitat Politècnica de Catalunya
Barcelona, Spain
pere.barlet@upc.edu*

Abstract—Network Intrusion Detection Systems (NIDS) are essential tools for detecting network attacks and intrusions. While extensive research has explored the use of supervised Machine Learning for attack detection and characterisation, these methods require accurately labelled datasets, which are very costly to obtain. Moreover, existing public datasets have limited and/or outdated attacks, and many of them suffer from mislabelled data. To reduce the reliance on labelled data, we propose AutoGraphAD, a novel unsupervised anomaly detection approach based on a Heterogeneous Variational Graph Autoencoder. AutoGraphAD operates on heterogeneous graphs, made from connection and IP nodes that capture network activity within a time window. The model is trained using unsupervised and contrastive learning, without relying on any labelled data. The reconstruction, structural loss, and KL divergence are then weighted and combined in an anomaly score that is then used for anomaly detection. Overall, AutoGraphAD yields the same, and in some cases better, results than previous unsupervised approaches, such as Anomal-E, but without requiring costly downstream anomaly detectors. As a result, AutoGraphAD achieves around 1.18 orders of magnitude faster training and 1.03 orders of magnitude faster inference, which represents a significant advantage for operational deployment.

Index Terms—Graph Neural Networks, Intrusion Detection System, Unsupervised Learning, Contrastive Learning, Graph Variational Autoencoders, Anomaly Detection

1. Introduction

In recent years, attacks and intrusions have been a growing problem. The attacks reported each year have been growing exponentially, with attacks becoming more and more sophisticated [1]. Thus, more robust Network Intrusion Detection Systems (NIDS) are needed to deal with the increasing volume and complexity of network attacks.

A substantial body of research has explored the use of Machine Learning (ML) to detect and characterise attacks [2]–[5]. However, most of these approaches are susceptible to adversarial attacks, and therefore do not suit real-life deployment [6]. Graph Neural Networks are known to be more robust against adversarial attacks, since they do not rely solely on network data, but also learn the structures and relationships among network traffic flows [7]–[9].

In the NIDS domain, the number of datasets that can be used to create and train ML models remains limited [10]. Most of these datasets use outdated attacks and are highly synthetic, creating a distorted image of how attacks are structured and work [11].

Labelling datasets is a costly and laborious task, which explains the scarcity of high-quality labelled data sets [12]. The main challenge is that each network flow must be examined and annotated by a domain expert, such as a Security Analyst [13]. This makes labelling large real-world network data almost impossible, which is why most research in this area relies on synthetic datasets [13].

Anomaly detection is a good approach to mitigate reliance on labelled datasets, as we only need normal data to establish a baseline, and anything that deviates from it is considered anomalous. In the domain of graph-based anomaly detection for NIDS, Anomal-E is arguably the most representative and influential approach [14]. Anomal-E constructs a homogeneous graph, where network flows are represented as edge features, which are then transformed to edge embeddings for anomaly detection. However, Anomal-E requires the generation of large embeddings, introducing significant overhead and slowing down the detection process [15]. Furthermore, in the case of concept drift [16], the entire pipeline has to be re-trained, making it computationally expensive to deploy in operational environments.

In the case of Anomal-E, and many other approaches [17]–[19], they rely on traditional downstream anomaly detection algorithms, which are often not suitable for a streaming environment [20], which makes them very difficult to deploy in real-world networks.

In this paper, we propose AutoGraphAD, a novel approach for unsupervised anomaly detection based on Variational Graph Autoencoders (VGAEs). In our approach, we represent network traffic as a heterogeneous graph with two distinct types of nodes, IP and Connection nodes. We then performed unsupervised contrastive training for the VGAE, without requiring any labelled data. We leverage the generated embeddings to calculate anomaly scores that are then used for anomaly detection. We have tested multiple different architectural variations to determine which implementation yields the best results at different levels of contamination (i.e., presence of anomalous flows) of the training dataset. AutoGraphAD yields the same, and in some cases better, results than Anomal-E while not relying on the use of costly downstream estimators. Thus, faster

training by 1.18 orders of magnitude and faster inference by 1.03 orders of magnitude is achieved, showcasing a significant advantage for operational deployment.

2. Problem Description

As mentioned in Section 1, the main problem that this paper aims to solve is the detection of network attacks without the need for expensive and limited labelled data. This is a very important problem that needs to be solved if we want to achieve more efficient results and a better real-life deployment of Machine Learning based NIDS.

The main issue with current solutions such as Anomal-E [14] and ARGANIDS [17] is the reliance on downstream detectors such as HBOS [21] to classify the embeddings generated for classification purposes. This adds an additional layer of computation that needs to be retuned often to account for concept drift [16] and the network's dynamic nature [20].

Moreover, certain one class classification algorithms tend to become prohibitively expensive when depending on the size of the embedding used. This can be seen in the case of OneClassSVM [22] and its linear variants, where the dimensionality of the features can negatively impact training and inference time, as well as memory complexity and overall performance [23]. It should be noted that, in the case of Anomal-E [14], the reported results use 256 vector embeddings. These embeddings can be considered large and affect anomaly detection algorithms as they suffer from the curse of dimensionality [15].

An interesting approach to avoid reliance on a downstream estimator is the use of dynamic Graph Autoencoders (VGAEs) to detect anomalies. This approach has been used successfully in network monitoring as seen in GAT-AD [24]. In the case of GAT-AD, the predicted and actual values are used to calculate an anomaly score, and then, based on those node scores, we can detect which nodes are anomalous and which are not.

In the case of anomaly detection in a network setting, the majority of state-of-the-art approaches rely on downstream estimators to conduct the anomaly detection.

In this paper, our aim is to achieve network detection without relying on a downstream detector. We rely solely on reconstruction errors and metrics and not on any other downstream detectors. We are aiming to leverage VGAEs and their reconstruction errors as a way to detect anomalous nodes. AutoGraphAD is substantially faster computationally than Anomal-E's and ARGANID's approaches, while much simpler and much more easily tunable.

3. Background

In this section, we describe the main pre-requisites of the technologies that we will be using in this paper as part of developing our solution.

3.1. Variational Graph Autoencoders

The underlying technology that we will use in this paper is VGAEs. VGAEs were originally proposed by Kipf in 2016 [25].

They are a Graph Neural Network extension of traditional Variational Autoencoders [26]. Their initial design relied on the reconstruction of the graph structure combined with the loss of Kullback-Leibler regularisation [25].

The variational autoencoder works by the encoder component creating uncertainty-aware node embeddings that are then parametrised into node embeddings and coupled with a Dot Product to recreate the Adjacency matrix of the graph [25]. Then both adjacency matrices are used to compute the reconstruction error. The equations used to calculate the errors can be seen in the following: Equation 1 is the Dot Product, Equation 2 is the Binary Cross Entropy Loss used to compute the structural reconstruction error [25], of Equation 3 is the KL regularisation error, and Equation 4 is the total loss used.

$$A' = Z \cdot Z^T \quad (1)$$

$$L_{Recon} = BCE(A', A) \quad (2)$$

$$KL_{Reg} = -\frac{1}{2} * \sum (1 + \log(\sigma^2) - \mu^2 - \sigma^2) \quad (3)$$

$$L_{Total} = L_{Recon} + KL_{Reg} \quad (4)$$

3.2. GraphSAGE

GraphSAGE is a Graph Neural Network architecture that can learn to generate embeddings from sampling and aggregating the node's neighbours [27]. After the aggregation, the generated embedding goes through a non-linear update.

The main advantage of GraphSAGE compared to other algorithms is that it can easily work with unseen nodes [27], making it ideal for real-time deployment where the nodes and graph structure differ from training data. In addition, GraphSAGE has been proven to scale very well in larger graphs [27], making it an ideal choice for a large network deployment.

3.3. Adversarially Regularised VGAEs

Adversarially Regularised VGAEs [28] is another approach to train the autoencoders to generate higher quality embeddings. This approach uses the exact same approach as the original VGAE paper [25] but adds the use of a regulariser model to improve the performance. The regulariser works by taking samples from the generated embeddings and from the a Gaussian distribution and learns to separate which one is which. This is then fed into the total loss that is used for back-propagation.

3.4. Multiple Sampling Variational Autoencoders

Another upgrade that can be done to enhance the VGAEs is through the use of multiple latent embeddings per node. The idea behind using multiple embeddings that are then used to reconstruct multiple reconstruction losses. This allows for the generation of an unbiased estimate of the same objective with a much smaller variance [29]. This has been proven to improve the performance of the model and yield better results [30].

3.5. KL Annealing

KL Annealing can be used to improve the performance of VAEs [31]. KL Annealing works by slowly increasing the KL regularisation loss through a set number of epochs. By slowly increasing the effect of the KL loss, the autoencoder is initially forced to learn meaningful embeddings, and then transitions on enforcing prior matching. The goal of this approach is to mitigate the posterior collapse, where KL transitions to 0, which can negatively affect the performance of the VAE.

3.6. Graph Masked Autoencoders

Masking was proposed by Hou et al. [32] in the Graph Masked Autoencoder (GraphMAE) and used in the Heterogenous Graph Masked Autoencoder (HGMAE) [33] to enhance the performance of their model. Their GAE architecture is enhanced by masking the input node features as well as the latent embeddings. Additionally, as part of model training, the graph edges are dropped. For masking, they use a learnable masking token similar to the one used in BERT [34]. Masking and edge dropping make it harder for the autoencoder to reconstruct the information, and thus the autoencoder does not learn trivial solutions during training but rather focusses on learning the node relations.

4. Methodology

In this section, we focus on describing our methodology and how we have created, trained, and evaluated AutoGraphAD. Additionally, we describe our pre-processing, graph-building, and dataset creation pipelines.

4.1. Dataset Used

For this work, we have chosen to use the UNSW-NB15 dataset [35]. We chose UNSW-NB15 for the AutoGraphAD evaluation, as it is a widely used dataset with clearly labelled modern attacks. Thus, our evaluation is better suited for the current environment. The data set has been generated from the raw PCAP files using NFStream [36]. For the generation of the flows, we used the same settings as were used in the original dataset generation. NFStream can output flows with multiple features. We chose the features that overlap with the features present in NetFlow V9 [37].

For UNSW-NB15, we used the generated labels from the original paper [35] and matched them with the flows generated by NFStream. The features used can be found in Table 5.

4.2. Dataset Creation

Having described the data pre-processing, it is important to describe how the datasets are created. The goal of this paper is to explore and showcase our model’s ability to detect anomalies even when the training data are contaminated. To achieve this, we have created different training parts with different levels of contamination similar to Anomal-E [14]. The main difference between

Anomal-E’s approach and ours is that Anomal-E uses 10% of the data set to create a single large graph for the training, and the same is repeated for testing. Our goal is to create 3 levels of contamination: No contamination, 3.5% Contamination, and 5.7% Contamination.

In our case, we use time windows to detect attacks and simulate a real-life deployment. For the training split of the dataset, we follow the following procedure; once we create all the sliding windows for the entire dataset, we calculate if the windows are anomalous or not, meaning if they contain attacks or not, and we do a stratified splitting to all datasets. For a training dataset that does not have any attacks, we removed all the anomalous graphs. For 3.5% contamination, we keep the stratified split, and for 5.7% we downsample the benign graphs for UNSW-NB15 as the normal contamination of the level is around 3.5%.

4.3. Feature Pre-processing and Graph Creation

For feature pre-processing, we use a similar pre-processing approach to the one proposed in Anomal-E [14]. The dataset is initially checked for flows with missing or infinite values, which are then removed. Following this step, we begin by building the time windows that will be used for training, testing, and evaluation. We then split the randomly generated graphs into parts for training, evaluation, and testing. We allocate 70% of the data for training, 20% for evaluation, and 10% for testing. For the time windows, we chose to create non-overlapping graphs that capture 180 seconds of traffic.

The second step of the pre-processing is feature normalisation. For categorical features, which in our case is the IP version and protocols, we employ One-Hot encoding [38]. In the case of the protocols, we use Rare Labelling from the library Feature Engine [39] due to the incredibly large number of protocols and the fact that the majority of these are very sparse in the data. Including these features in One-Hot encoding would increase the dimensionality of the data without yielding any performance gain; as such, the rarer protocols are bundled in a third category labelled Rare, resulting in three One-Hot categories, two for the two most common features, and one for all the rare features.

For the continuous features, we are using L2 row wise normalisation. This choice was made because it does not require any significant pre-processing and can be done on the fly in a real-life environment, allowing for an easier real-life deployment. The entire process from dataset creation to graph creation can be seen in Figure 1.

4.4. Network Architecture and Variants

Our proposed architecture builds upon the original VGAE [25] and extends it by incorporating elements from GraphMAE [32] and HGMAE [33]. Our architecture is designed to reconstruct both node features and graph structure during training. The main upgrades introduced in our design are as follows.

We are using the same masking component as used in GraphMAE [32] and HGMAE [33], but instead of masking both latent embeddings and original graph embeddings, we only mask the original graph nodes. We

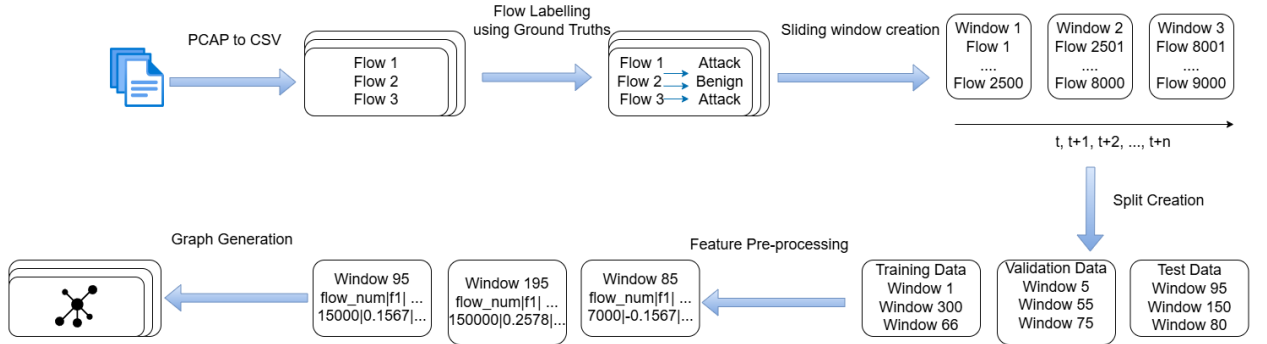


Figure 1. Dataset Pre-processing pipeline for graph generation

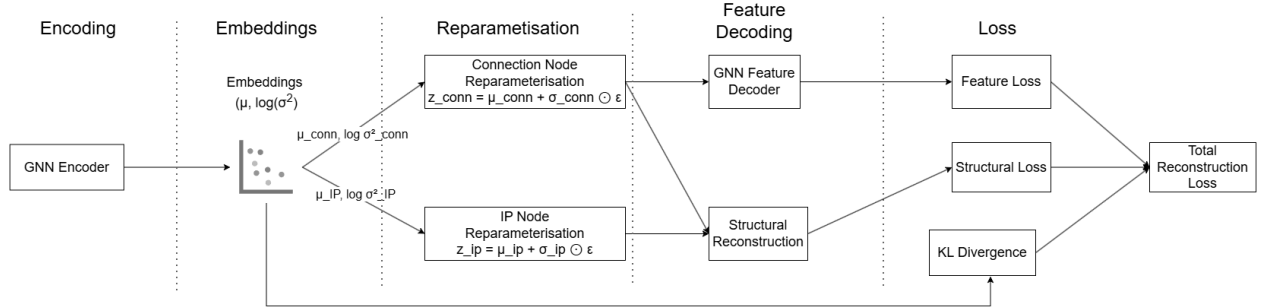


Figure 2. The proposed Architecture of AutoGraphAD in a training setting. AutoGraphAD mainly focuses on the reconstruction and use of the connection nodes as the IP nodes have placeholder values. The pipeline starts with the encoder that generates the latent space embeddings that are then reparametrised to create the embeddings that are then used for structure and feature reconstruction. Using the reconstructed values, we calculate the reconstruction losses used for back-propagation. The GNN encoder and decoder can be switched out with every other GNN algorithm. The same can be done regarding the losses that are used in Back-propagation.

made this decision because during the evaluation of AutoGraphAD there was a negligible improvement when using double masking.

We incorporated random edge drop during training to force the model to learn non-trivial relationships between nodes [33]. We have also incorporated negative edge sampling as a contrastive learning objective to help the autoencoder to better distinguish between real and fake edges. This helps our autoencoder to learn better the structure of the graphs.

For structural reconstruction, we use an enhanced Dot Product. The enhanced Dot Product uses learnable weights to better capture the structural dependencies of the graphs. This is because a heterogeneous graph can be split into smaller bipartite graphs [40]. This allows us to assign a learnable weight for each of the edge types and better capture that individual relationship. For the structural reconstruction error, we use Binary Cross entropy loss as seen in the original VGAE paper [25].

$$A' = Z \cdot (W * Z^T) \quad (5)$$

Regarding feature reconstruction, a GNN has been employed to decode the node features. A GNN was chosen as it is the most capable of decoding the embeddings correctly. GNNs as a decoder are used in both HGMAE and GraphMAE [32], [33], but in these approaches they have focused only on decoding masked embeddings. In

this architecture, all nodes are decoded. In our approach, we only decode the connection nodes as the IP nodes are placeholder values that do not contain any meaningful information.

Regarding the feature reconstruction errors, we have created two main variants, one using the Cosine Embedding Error and one using the Mean Squared Error (MSE). The Cosine Embedding Error approach has been inspired by HGMAE [33] and GraphMAE [32], while the MSE approach has been chosen as the goal here of the autoencoder is to be able to generate meaningful embeddings in which the decoded values must be closest to the actual values. The KL divergence loss used in our model is the same as in the original VGAE paper [25].

For the total reconstruction loss, we combine the feature reconstruction loss with the structural reconstruction loss and KL divergence. The total loss is then back-propagated through the model to update the model. Each component of the total reconstruction loss, with the exception of the KL divergence, is weighted by a user defined value. The model architecture can be found in Figure 2 and the total loss is depicted in equation 6.

$$L_{Total} = \alpha * L_{Structure} + \beta * L_{Features} + KL \quad (6)$$

4.5. Model Training

The model was trained with 100 maximum allowable epochs. We used an early stopping mechanism during the training to prevent overfitting and expenditure of the computational resources. Furthermore, we saved the model’s weights at the point that the model achieved its best performance. We ensured that we maintain the optimal version of the model.

4.6. Anomaly Detection

For anomaly detection, we are calculating the anomaly scores of the connection nodes. The anomaly scores are based on the calculation of the reconstruction errors with the KL term. The idea is that the anomaly score will be lower for normal nodes and higher for anomalous nodes. To determine the threshold of what an anomaly is and what it is not, we use percentiles to determine a user defined percentile, and then everything above it is determined as anomalous scores. For our score, we use the following equation.

$$Score = \alpha * L_{Feat} + \beta * L_{Struct} + \gamma * KL \quad (7)$$

The equation works by using a user-assigned score to weight the importance of each loss in the anomaly score. This allows us to use different weights for different settings. Additionally, we employ Robust Scaling [41] of all reconstruction errors and KL Divergence that are used for the anomaly scores. This guarantees that all scores are on the same scale and that no value dominates the range and skews the anomaly scores [42]. Our entire approach runs in PyTorch and on the GPU. Providing a faster processing time than using Sci-kit learn [23]. The pipeline can be found in Figure 9 in the Appendix.

4.7. Evaluating Inference Performance

To evaluate the performance of each method, we have chosen to measure the training and inference times. For timing, we used the Python built-in library, time. More specifically, we used the function `perf_counter_ns()` which gives us the most accurate measurement for our experiment, since we are measuring short durations.

For timing, we do not count the parts where data transfer takes place to make the comparisons more equal. Moreover, in the case of AutoGraphAD, we can time each individual pass when generating the Anomaly Score, but this is not possible during threshold setting and threshold inference timing and when timing Anomal-E’s downstream estimator training and inference. For these cases, we get the total time and divide it based on the number of graphs that were processed.

For the recorded timings, in the case of AutoGraphAD we add the average time per graph during the anomaly score with its respective time in the threshold component. For example, in the case of the training time, we add the average anomaly score generation time per graph with the estimated threshold calculation time per graph.

4.8. Libraries Used

To create our VGAE, we used PyTorch [43] and an extension of PyTorch called PyTorch Geometric [44] which is best suited for the creation and training of GNNs. To ensure easier reproducibility and faster training, we employed PyTorch Lightning [45]. Regarding anomaly detection, we employed NumPy [46] and PyOD [47]. Finally, for data pre-processing, window creation, and running the downstream tasks for Anomal-E, we used Scikit-learn [23] and Pandas [48]. To run the Anomal-E code we used DGL [49].

5. Experimental Results

5.1. Experimental setup

To evaluate AutoGraphAD, we used UNSW-NB15 in both AutoGraphAD and Anomal-E. For Anomal-E, we used an implementation found in a GitHub repository¹.

Overall, we trained the models in the different contamination levels² followed by the anomaly detection estimators’ grid search for Anomal-E and weight search for the Anomaly Score in the VGAE implementation. During the hyperparameter search, the model weights were frozen.

To run our experiments, we used a server with an Nvidia RTX 3090 with 24 GB of VRAM. The CPU of the server is an AMD Ryzen 3950X, 16-Core Processor. The server came with 64 GB of RAM and its operating system was Ubuntu 22.04.4 LTS.

5.2. VGAE Variants

We exhaustively tested multiple different VGAE variants. Our base architecture is node masking and edge dropping to force the variational autoencoders to learn non-trivial node relationships. The variants that we evaluated are the following: (1) Base architecture using MSE for node feature reconstruction, (2) Base architecture using Cosine Embedding Error for node feature reconstruction, (3) Regularised Base Architecture, (4) Split Base Architecture, and (5) Multiple Sampling Base Architecture.

On top of all of these architectures, we additionally evaluated each version using 1 and 2 layer encoders and decoders, as well as using KL annealing.

5.3. Training Hyperparameters

For training the Anomal-E dataset we used the hyperparameters present in the GitHub’s repository. These were verified to be the same hyperparameters as those mentioned in the original paper [14].

For AutoGraphAD, we have run multiple versions of our architecture. We have run different versions with different upgrades to evaluate which yields the best results. A summary of the different settings we used can be found in Table 1.

1. <https://github.com/waimorris/Anomal-E>

2. The contamination level indicates the percentage of anomalous flows present in the training set. Ideally, anomaly detection methods should be trained only on normal flows. However, this is difficult to guarantee in real-world environments. Hence, robustness to a small degree of contamination is desirable for practical deployment in operational networks.

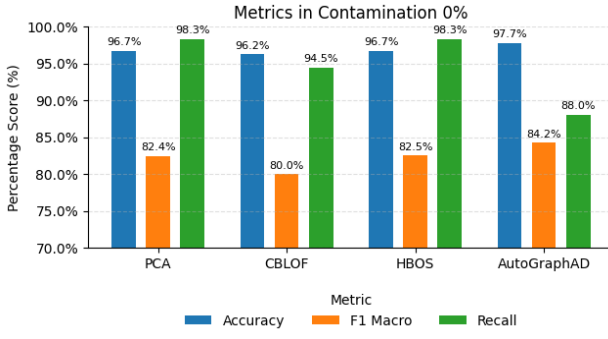


Figure 3. Performance metrics in 0% training dataset.

Hyperparameter	Hyperparameter Values
No. Layers	[1, 2]
No. Hidden	32
Learning Rate	1e-3
Activation Function	ReLU
Loss Function for Structural Loss	Binary Cross Entropy
Loss Function for Feature Loss	[Mean Square Error, Cosine Embedding Loss]
Optimiser	AdamW
Weight Decay	1e-5
KL Annealing	[Yes, No]
KL Annealing Epochs	10
KL Min Weight	0.0
Regulariser	[Yes, No]
Multiple Draw	[Yes, No]
Maximum Epochs	100
Early Stop Patience	20
Feature Importance	1.0
Structural Importance	1.0

TABLE 1. AUTOGRAPHAD HYPERPARAMETERS

5.4. Anomaly Detection Hyperparameters

For Anomal-E to work for anomaly detection, it requires a downstream detector to characterise attacks as anomalies or not. In the case of Anomal-E we chose to use the same algorithms as they used in their original paper [14]. These algorithms are PCA, CBLOF, and HBOS. For the Hyperparameter search, we used a more extensive search than what was used in the original paper; a summary of the Hyperparameter search can be seen in Table 2.

Hyperparameter	Hyperparameter Values
PCA no. components	[0.96, 0.98, 0.99]
PCA Weighted	True
PCA Whiten	[True, False]
PCA Standardisation	True
HBOS Bins	[5, 6, 8, 10, 12, 14, 16, 18, 20]
HBOS Alpha	[0.05, 0.1]
HBOS Tol	[0.1, 0.5]
Contamination (Anomal-E)	[0.02, 0.035, 0.05, 0.1, 0.2]
Alpha (AutoGraphAD)	[0.1, 0.5, 1.0]
Beta (AutoGraphAD)	[0.1, 0.5, 1.0]
Gamma (AutoGraphAD)	[0.1, 0.5, 1.0]
MSE use (AutoGraphAD)	[True, False]
Percentile (AutoGraphAD)	[95, 97, 98, 99]

TABLE 2. ANOMAL-E ESTIMATOR AND AUTOGRAPHAD ANOMALY SCORE HYPERPARAMETERS

For AutoGraphAD, we have tried different settings to

find the combination that yields the most reliable anomaly scores. As mentioned in Section 4, we have individually configurable weights that affect the anomaly score. A detailed summary of the different parameters that we have evaluated can be found in Table 2.

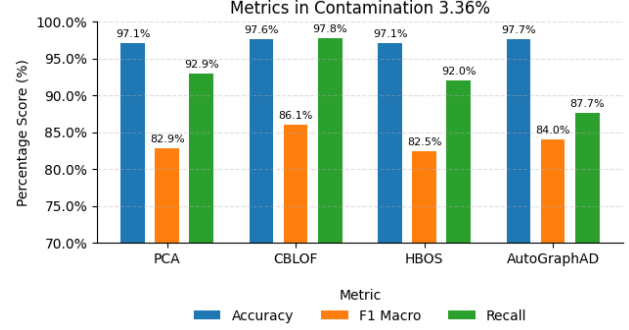


Figure 4. Performance metrics at 3.36% contamination in the training dataset.

5.5. Results and interpretation

For the results, we have chosen the best of our variants for each level of contamination and different weights for the anomaly score. The model hyperparameters, anomaly score weights can be found in Tables 7 and 8 in the Appendix. The metrics used are Accuracy, F1 Macro and Recall Macro. These metrics were chosen as an accurate descriptor of the model’s performance and because Macro treats each class as equal [52], whereas other types of results do not, making them ideal for evaluating the model in a highly unbalanced dataset like UNSW-Nb15 [35].

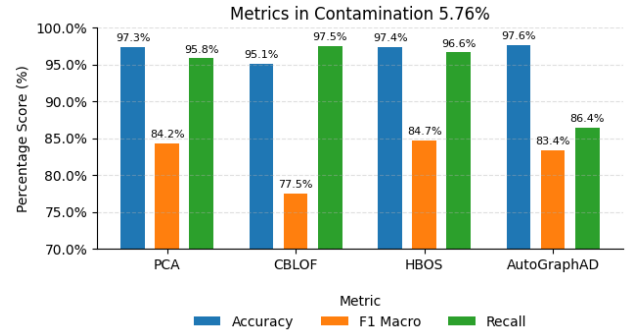


Figure 5. Performance metrics of all the approaches at 5.76% contamination.

Figures 3, 4, and 5 show the results of our experimental evaluation for the different levels of contamination. AutoGraphAD yields very good results, comparable to those of Anomal-E. It should be noted that AutoGraphAD does not rely on any downstream anomaly detection algorithms such as Anomal-E, making it ideal for real-life deployment, as it can be tuned and adjusted more easily rather than requiring training on the new dataset. Furthermore, it should be noted that Anomal-E uses embeddings of size 256 [14] whereas we rely on embeddings of size 32, 32 for the mean, and 32 for the Log Variance.

Our results at 0% contamination exceed Anomal-E’s, especially when it comes to accuracy and F1 results.

TABLE 3. RESULTS OF ANOMAL-E AND AUTOGRAPHAD

Metrics	0% Contamination			3.36% Contamination			5.76% Contamination		
	Accuracy	F1	Recall	Accuracy	F1	Recall	Accuracy	F1	Recall
PCA (Anomal-E)	96.65%	82.39%	98.27%	97.3%	82.56%	95.81%	97.13%	84.24%	92.95%
CBLOF (Anomal-E)	96.21%	79.96%	94.46%	95.11%	77.51%	97.47%	97.63%	86.05%	97.76%
HBOS (Anomal-E)	96.68%	82.5%	98.28%	97.37%	84.73%	96.61%	97.1%	82.48%	91.97%
Anomaly Score (AutoGraphAD)	97.69%	84.23%	87.98%	97.67%	84.03%	87.67%	97.6%	83.36%	86.42%

Anomal-E seems to be performing better in Recall, but looking at the F1 score its Precision seems to be lower than AutoGraphAD, indicating a higher false positive count than our own approach. This continues in the case of the 3.36% contamination level, where only CBLOF seems to perform better than AutoGraphAD. In the case of 5.76% contamination levels, again we achieve higher results with the exception of Recall against most of Anomal-E's estimators with the exception of HBOS.

It is worth noting that the size of our embeddings is eight times smaller than those used by Anomal-E. This reduction is especially important for methods that use a downstream detector, because smaller embeddings can significantly improve both performance and processing speeds [15].

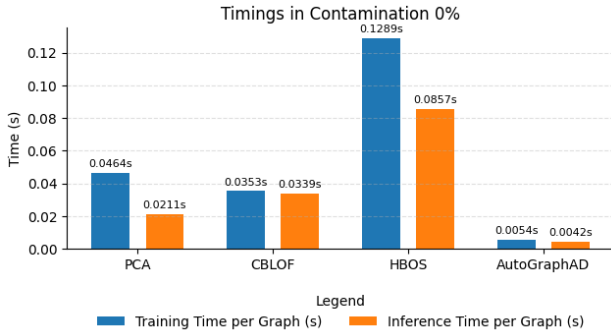


Figure 6. Timing for inference and training in Seconds at 0% contamination in the training dataset.

AutoGraphAD yields substantially better inference time as seen in Table 4 and Figures 6, 7, and 8. This can mainly be attributed to the fact that AutoGraphAD is GPU native, as it does not require a downstream detector as Anomal-E, allowing for faster parallelisation and less time and resources spent on memory transfers to the CPU Anomal-E's estimators.

Furthermore, AutoGraphAD is capable of being more easily tuned by just adjusting the weight parameters of the anomaly score, making alterations on the anomaly score generation on the fly. Unfortunately, this cannot truly be

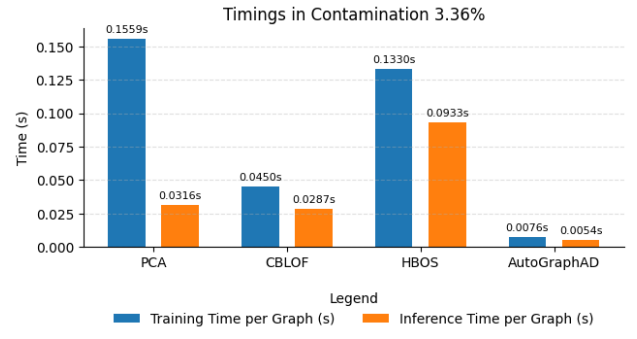


Figure 7. The timings for training and inference at 3.36% contamination.

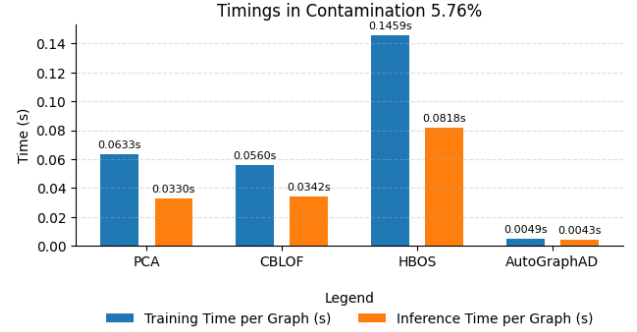


Figure 8. The timings for training and inference at 5.76% contamination.

done in the case of the estimators as their characteristics are set during initialisation. Some of the estimator thresholds may be manually adjusted [47] [23], but this is also the case in AutoGraphAD. Finally, in the case of model retuning or retraining, Anomal-E's estimators need to be re-trained from the start as the PyOD's architecture does not support retuning [47]. Instead, in our case, it is very easy to retune both the model and the anomaly score, since attacks are determined from a percentile threshold that is relatively lightweight in terms of inference and training. It should be noted that the use of Robust Scaling for each sliding window's errors allows the model to

TABLE 4. TIME MEASUREMENT OF THE ANOMAL-E'S DOWNSTREAM ESTIMATORS AND AUTOGRAPHAD. ALL TIMES ARE THE AVERAGE FROM ALL THE CONTAMINATION LEVELS AND ARE THE TIME PER GRAPH.

Estimator	Training (s)	Inference (s)	Anomaly Score calculation (s)	Threshold calculation (s)	Threshold inference (s)
PCA [50]	0.0885	0.0286	—	—	—
CBLOF [51]	0.0454	0.0323	—	—	—
HBOS [21]	0.1359	0.0869	—	—	—
AutoGraphAD	0.0060	0.0046	0.00529	0.000015	0.000002

be more resilient to anomalies, since extreme values do not dominate scaling [41]. Finally, traditional anomaly detection methods are not the best when it comes to streaming environments such as NIDS [20], whereas AutoGraphAD scales each graph on its own and its thresholds and anomaly score weights can be easily retuned on the fly. This makes it an ideal candidate for an NIDS system.

6. Conclusion

In conclusion, AutoGraphAD leverages recent advancements in the space of GVAEs and GAEs [25], [28], [32], [33] to build a more practical approach for network anomaly detection. Our design is relatively simple and yields results comparable to those of the Anomal-E. The main advantage of AutoGraphAD is faster inference and detection times, lower number of false positives, and easier and faster pipeline retuning than Anomal-E's approach.

Furthermore, our evaluation allowed us to further explore the importance of node masking, negative edge sampling, and edge dropping. Our results highlight that lower masking, edge sampling, and edge dropping work better when we have very little or substantial contamination on our training graphs, whereas they seem more important when contamination is the same as with the rest of the dataset splits. This provides us with more information on how to tune our models for different training and inference conditions.

Our future work will focus on evaluating the generalisation capabilities of our model across unseen network scenarios, including a broader range of datasets. Assessing the capacity of a model to operate in a different environment than those seen in training is also essential to ensure practical deployment in operational networks.

Acknowledgements

This work was supported by Grant PCI2023-145974-2 funded by MICIU/AEI/10.13039/501100011033 and co-funded by the European Union (GRAPHS4SEC project).

GitHub Copilot was used to help debug and develop the code. It served mainly as a search engine for what was causing the bugs and as a recommendation engine to check which libraries and their methods are the most suitable and optimal during development.

References

- [1] S. Kumar, S. Gupta, and S. Arora, “Research trends in network-based intrusion detection systems: A review,” *IEEE Access*, vol. 9, pp. 157 761–157 779, 2021.
- [2] W. Wang, Y. Sheng, J. Wang, X. Zeng, X. Ye, Y. Huang, and M. Zhu, “Hast-ids: Learning hierarchical spatial-temporal features using deep neural networks to improve intrusion detection,” *IEEE Access*, vol. 6, pp. 1792–1806, 2018.
- [3] S. Zaman and F. Karray, “Lightweight ids based on features selection and ids classification scheme,” in *2009 International Conference on Computational Science and Engineering*, vol. 3, 2009, pp. 365–370.
- [4] B. Babu, G. Reddy, D. Goud, K. Naveen, and K. T. Reddy, “Network intrusion detection using machine learning algorithms,” in *2023 3rd International Conference on Smart Data Intelligence (ICSDI)*, 2023, pp. 367–371.
- [5] R. Chapaneri and S. Shah, “A comprehensive survey of machine learning-based network intrusion detection,” in *Smart Intelligent Computing and Applications*, S. C. Satapathy, V. Bhateja, and S. Das, Eds. Singapore: Springer Singapore, 2019, pp. 345–356.
- [6] N. Papernot, P. McDaniel, S. Jha, M. Fredrikson, Z. B. Celik, and A. Swami, “The limitations of deep learning in adversarial settings,” in *2016 IEEE European Symposium on Security and Privacy (EuroS&P)*, 2016, pp. 372–387.
- [7] D. Pujol-Perich, J. Suárez-Varela, A. Cabellos-Aparicio, and P. Barlet-Ros, “Unveiling the potential of graph neural networks for robust intrusion detection,” 2021. [Online]. Available: <https://arxiv.org/abs/2107.14756>
- [8] T. Bilot, N. E. Madhoun, K. A. Agha, and A. Zouaoui, “Graph neural networks for intrusion detection: A survey,” *IEEE Access*, vol. 11, pp. 49 114–49 139, 2023.
- [9] Z. Sun, A. M. Teixeira, and S. Toor, “Gnn-ids: Graph neural network based intrusion detection system,” in *Proceedings of the 19th International Conference on Availability, Reliability and Security*, ser. ARES ’24. New York, NY, USA: Association for Computing Machinery, 2024. [Online]. Available: <https://doi.org/10.1145/3664476.3664515>
- [10] P. Goldschmidt and D. Chudá, “Network intrusion datasets: A survey, limitations, and recommendations,” 2025. [Online]. Available: <https://arxiv.org/abs/2502.06688>
- [11] D. Pinto, I. Amorim, E. Maia, and I. Praça, “A review on intrusion detection datasets: tools, processes, and features,” *Computer Networks*, vol. 262, p. 111177, 2025. [Online]. Available: <https://www.sciencedirect.com/science/article/pii/S1389128625001458>
- [12] T. Braun, I. Pekaric, and G. Apruzzese, “Understanding the process of data labeling in cybersecurity,” in *Proceedings of the 39th ACM/SIGAPP Symposium on Applied Computing*, ser. SAC ’24. ACM, Apr. 2024, p. 1596–1605. [Online]. Available: <http://dx.doi.org/10.1145/3605098.3636046>
- [13] J. L. Guerra, C. Catania, and E. Veas, “Datasets are not enough: Challenges in labeling network traffic,” *Computers & Security*, vol. 120, p. 102810, 2022. [Online]. Available: <https://www.sciencedirect.com/science/article/pii/S0167404822002048>
- [14] E. Caville, W. W. Lo, S. Layeghy, and M. Portmann, “Anomal-e: A self-supervised network intrusion detection system based on graph neural networks,” *Knowledge-Based Systems*, vol. 258, p. 110030, Dec. 2022. [Online]. Available: <http://dx.doi.org/10.1016/j.knosys.2022.110030>
- [15] R. Bellman, “Dynamic programming,” *Science*, vol. 153, no. 3731, pp. 34–37, 1966. [Online]. Available: <https://www.science.org/doi/abs/10.1126/science.153.3731.34>
- [16] G. I. Webb, R. Hyde, H. Cao, H. L. Nguyen, and F. Petitjean, “Characterizing concept drift,” *Data Min. Knowl. Discov.*, vol. 30, no. 4, pp. 964–994, Jul. 2016.
- [17] A. Venturi, M. Ferrari, M. Marchetti, and M. Colajanni, “Arganids: a novel network intrusion detection system based on adversarially regularized graph autoencoder,” in *Proceedings of the 38th ACM/SIGAPP Symposium on Applied Computing*, ser. SAC ’23. New York, NY, USA: Association for Computing Machinery, 2023, p. 1540–1548. [Online]. Available: <https://doi.org/10.1145/3555776.3577651>
- [18] A. Zoubir and B. Missaoui, “Integrating graph neural networks with scattering transform for anomaly detection,” 2024. [Online]. Available: <https://arxiv.org/abs/2404.10800>
- [19] Q. Xiao, J. Liu, Q. Wang, Z. Jiang, X. Wang, and Y. Yao, “Towards network anomaly detection using graph embedding,” in *Computational Science – ICCS 2020*, V. V. Krzhizhanovskaya, G. Závodszky, M. H. Lees, J. J. Dongarra, P. M. A. Sloot, S. Brissos, and J. Teixeira, Eds. Cham: Springer International Publishing, 2020, pp. 156–169.
- [20] T. Lu, L. Wang, and X. Zhao, “Review of anomaly detection algorithms for data streams,” *Applied Sciences*, vol. 13, no. 10, 2023. [Online]. Available: <https://www.mdpi.com/2076-3417/13/10/6353>
- [21] M. Goldstein and A. Dengel, “Histogram-based outlier score (hbos): A fast unsupervised anomaly detection algorithm,” in *KI 2012: Poster and Demo Track*, 2012, pp. 59–63. [Online]. Available: <https://www.goldiges.de/publications/HBOS-KI-2012.pdf>

[22] B. Schölkopf, R. C. Williamson, A. Smola, J. Shawe-Taylor, and J. Platt, "Support vector method for novelty detection," in *Advances in Neural Information Processing Systems*, S. Solla, T. Leen, and K. Müller, Eds., vol. 12. MIT Press, 1999. [Online]. Available: https://proceedings.neurips.cc/paper_files/paper/1999/file/8725fb777f25776ffa9076e44fcfd776-Paper.pdf

[23] F. Pedregosa, G. Varoquaux, A. Gramfort, V. Michel, B. Thirion, O. Grisel, M. Blondel, P. Prettenhofer, R. Weiss, V. Dubourg, J. Vanderplas, A. Passos, D. Cournapeau, M. Brucher, M. Perrot, and E. Duchesnay, "Scikit-learn: Machine learning in Python," *Journal of Machine Learning Research*, vol. 12, pp. 2825–2830, 2011.

[24] H. Latif-Martínez, J. Suárez-Varela, A. Cabellos-Aparicio, and P. Barlet-Ros, "Gat-ad: Graph attention networks for contextual anomaly detection in network monitoring," *Computers & Industrial Engineering*, vol. 200, p. 110830, 2025. [Online]. Available: <https://www.sciencedirect.com/science/article/pii/S0360835224009525>

[25] T. N. Kipf and M. Welling, "Variational graph auto-encoders," 2016. [Online]. Available: <https://arxiv.org/abs/1611.07308>

[26] D. P. Kingma and M. Welling, "Auto-encoding variational bayes," 2022. [Online]. Available: <https://arxiv.org/abs/1312.6114>

[27] W. Hamilton, Z. Ying, and J. Leskovec, "Inductive representation learning on large graphs," in *Advances in Neural Information Processing Systems*, I. Guyon, U. V. Luxburg, S. Bengio, H. Wallach, R. Fergus, S. Vishwanathan, and R. Garnett, Eds., vol. 30. Curran Associates, Inc., 2017. [Online]. Available: https://proceedings.neurips.cc/paper_files/paper/2017/file/5dd9db5e033da9c6fb5ba83c7a7ebea9-Paper.pdf

[28] S. Pan, R. Hu, G. Long, J. Jiang, L. Yao, and C. Zhang, "Adversarially regularized graph autoencoder for graph embedding," 2019. [Online]. Available: <https://arxiv.org/abs/1802.04407>

[29] A. Mnih and D. Rezende, "Variational inference for monte carlo objectives," in *Proceedings of The 33rd International Conference on Machine Learning*, ser. Proceedings of Machine Learning Research, M. F. Balcan and K. Q. Weinberger, Eds., vol. 48. New York, New York, USA: PMLR, 20–22 Jun 2016, pp. 2188–2196. [Online]. Available: <https://proceedings.mlr.press/v48/mnihb16.html>

[30] A. Buchholz, F. Wenzel, and S. Mandt, "Quasi-Monte Carlo variational inference," in *Proceedings of the 35th International Conference on Machine Learning*, ser. Proceedings of Machine Learning Research, J. Dy and A. Krause, Eds., vol. 80. PMLR, 10–15 Jul 2018, pp. 668–677. [Online]. Available: <https://proceedings.mlr.press/v80/buchholz18a.html>

[31] S. Bowman, L. Vilnis, O. Vinyals, A. Dai, R. Jozefowicz, and S. Bengio, "Generating sentences from a continuous space," in *Proceedings of the 20th SIGNLL conference on computational natural language learning*, 2016, pp. 10–21.

[32] Z. Hou, X. Liu, Y. Cen, Y. Dong, H. Yang, C. Wang, and J. Tang, "Graphmae: Self-supervised masked graph autoencoders," in *Proceedings of the 28th ACM SIGKDD Conference on Knowledge Discovery and Data Mining*, ser. KDD '22. New York, NY, USA: Association for Computing Machinery, 2022, p. 594–604. [Online]. Available: <https://doi.org/10.1145/3534678.3539321>

[33] Y. Tian, K. Dong, C. Zhang, C. Zhang, and N. V. Chawla, "Heterogeneous graph masked autoencoders," 2023. [Online]. Available: <https://arxiv.org/abs/2208.09957>

[34] J. Devlin, M.-W. Chang, K. Lee, and K. Toutanova, "Bert: Pre-training of deep bidirectional transformers for language understanding," 2019. [Online]. Available: <https://arxiv.org/abs/1810.04805>

[35] N. Moustafa and J. Slay, "Unsw-nb15: a comprehensive data set for network intrusion detection systems (unsw-nb15 network data set)," in *2015 Military Communications and Information Systems Conference (MilCIS)*, 2015, pp. 1–6.

[36] Z. Aouini and A. Pekar, "Nfstream: A flexible network data analysis framework," *Computer Networks*, vol. 204, p. 108719, 2022. [Online]. Available: <https://www.sciencedirect.com/science/article/pii/S1389128621005739>

[37] B. Claise, "Cisco systems netflow services export version 9," Cisco, Tech. Rep., 2004.

[38] J. T. Hancock and T. M. Khoshgoftaar, "Survey on categorical data for neural networks," *Journal of Big Data*, vol. 7, no. 1, Apr. 2020. [Online]. Available: <http://dx.doi.org/10.1186/s40537-020-00305-w>

[39] S. Galli, "Feature-engine: A python package for feature engineering for machine learning," *Journal of Open Source Software*, vol. 6, no. 65, p. 3642, 2021. [Online]. Available: <https://doi.org/10.21105/joss.03642>

[40] C. Shi, X. Wang, and P. S. Yu, *The State-of-the-Art of Heterogeneous Graph Representation*. Singapore: Springer Singapore, 2022, pp. 9–25. [Online]. Available: https://doi.org/10.1007/978-981-16-6166-2_2

[41] P. J. Rousseeuw and M. Hubert, "Anomaly detection by robust statistics," *WIREs Data Mining and Knowledge Discovery*, vol. 8, no. 2, p. e1236, 2018. [Online]. Available: <https://wires.onlinelibrary.wiley.com/doi/abs/10.1002/widm.1236>

[42] A. Zimek, R. J. Campello, and J. Sander, "Ensembles for unsupervised outlier detection: challenges and research questions a position paper," *SIGKDD Explor. Newsl.*, vol. 15, no. 1, p. 11–22, Mar. 2014. [Online]. Available: <https://doi.org/10.1145/2594473.2594476>

[43] A. Paszke, S. Gross, F. Massa, A. Lerer, J. Bradbury, G. Chanan, T. Killeen, Z. Lin, N. Gimelshein, L. Antiga, A. Desmaison, A. Kopf, E. Yang, Z. DeVito, M. Raison, A. Tejani, S. Chilamkurthy, B. Steiner, L. Fang, J. Bai, and S. Chintala, "Pytorch: An imperative style, high-performance deep learning library," in *Advances in Neural Information Processing Systems*, H. Wallach, H. Larochelle, A. Beygelzimer, F. d'Alché-Buc, E. Fox, and R. Garnett, Eds., vol. 32. Curran Associates, Inc., 2019. [Online]. Available: https://proceedings.neurips.cc/paper_files/paper/2019/file/dbca288fee7f92f2bfa9f7012727740-Paper.pdf

[44] M. Fey and J. E. Lenssen, "Fast graph representation learning with pytorch geometric," 2019. [Online]. Available: <https://arxiv.org/abs/1903.02428>

[45] W. Falcon and The PyTorch Lightning team, "Pytorch lightning," March 2019. [Online]. Available: <https://github.com/Lightning-AI/lightning>

[46] C. R. Harris, K. J. Millman, S. J. van der Walt, R. Gommers, P. Virtanen, D. Cournapeau, E. Wieser, J. Taylor, S. Berg, N. J. Smith, R. Kern, M. Picus, S. Hoyer, M. H. van Kerkwijk, M. Brett, A. Haldane, J. F. del Río, M. Wiebe, P. Peterson, P. Gérard-Marchant, K. Sheppard, T. Reddy, W. Weckesser, H. Abbasi, C. Gohlke, and T. E. Oliphant, "Array programming with NumPy," *Nature*, vol. 585, no. 7825, pp. 357–362, Sep. 2020. [Online]. Available: <https://doi.org/10.1038/s41586-020-2649-2>

[47] Y. Zhao, Z. Nasrullah, and Z. Li, "Pyod: A python toolbox for scalable outlier detection," *Journal of Machine Learning Research*, vol. 20, no. 96, pp. 1–7, 2019. [Online]. Available: <http://jmlr.org/papers/v20/19-011.html>

[48] Wes McKinney, "Data Structures for Statistical Computing in Python," in *Proceedings of the 9th Python in Science Conference*, Stéfan van der Walt and Jarrod Millman, Eds., 2010, pp. 56 – 61.

[49] M. Wang, D. Zheng, Z. Ye, Q. Gan, M. Li, X. Song, J. Zhou, C. Ma, L. Yu, Y. Gai, T. Xiao, T. He, G. Karypis, J. Li, and Z. Zhang, "Deep graph library: A graph-centric, highly-performant package for graph neural networks," 2020. [Online]. Available: <https://arxiv.org/abs/1909.01315>

[50] Y. Zhao and P. contributors. (2025) pyod.models.pca — pyod 2.0.5 documentation. Source code and API notes for the PCA outlier detector; BSD-2-Clause. [Online]. Available: https://pyod.readthedocs.io/en/latest/_modules/pyod/models/pca.html

[51] Z. He, X. Xu, and S. Deng, "Discovering cluster-based local outliers," *Pattern Recognition Letters*, vol. 24, no. 9, pp. 1641–1650, 2003. [Online]. Available: <https://www.sciencedirect.com/science/article/pii/S0167865503000035>

[52] M. Du, N. Tatbul, B. Rivers, A. K. Gupta, L. Hu, W. Wang, R. Marcus, S. Zhou, I. Lee, and J. Gottschlich, "A skew-sensitive evaluation framework for imbalanced data classification," 2023. [Online]. Available: <https://arxiv.org/abs/2010.05995>

Appendix

TABLE 5. NETFLOW DATASET FEATURE SET

#	Column name	Feature	Value	NF (v9)
1	src ip	Source IP address	Str	Yes
2	src port	Source Port	Int	Yes
3	dst ip	Destination IP address	Str	Yes
4	protocol	Destination port	Int	Yes
5	ip version	IP version	Int	Yes
6	bidirectional first seen ms	Timestamp in milliseconds of the first seen packet of the flow	Int	Yes
7	bidirectional last seen ms	Timestamp in milliseconds of the last seen packet of the flow	Int	Yes
8	bidirectional duration ms	Duration of the entire flow in milliseconds	Int	Yes
9	bidirectional packets	Total packets of the flow	Int	Yes
10	bidirectional bytes	Total bytes of the flow	Int	Yes
11	bidirectional min packet size	Minimum packet size of the flow	Int	Yes
12	bidirectional max packet size	Maximum packet size of the flow	Int	Yes
13	bidirectional mean packet size	Mean of the size of the packet flows	Float	Yes
14	bidirectional mean packet iat ms	Mean of the inter arrival packet time of all the packets of the flow in milliseconds	Float	Yes
15	bidirectional cumulative flags	Logical OR of the flags of all the packets of the flow	Int	Yes
16	src2dst first seen ms	Timestamp in milliseconds of the first seen packet from source to destination IP address	Int	Yes
17	src2dst last seen ms	Timestamp in milliseconds of the last seen packet from source to destination IP address	Int	Yes
18	src2dst duration ms	Total duration of the source to destination packets in milliseconds	Int	Yes
19	src2dst packets	Total packets sent from source to destination IP address	Int	Yes
20	src2dst bytes	Total bytes sent from source to destination IP address	Int	Yes
21	src2dst min packet size	Minimum packet size sent from source to destination IP address	Int	Yes
22	src2dst max packet size	Maximum packet size sent from source to destination IP address	Int	Yes
23	src2dst mean packet size	Mean of the size of the packets sent from source to destination IP address	Float	Yes
24	src2dst mean packet iat ms	Mean of the inter arrival packet time of all the packets sent from source to destination IP address in milliseconds	Float	Yes
25	src2dst cumulative flags	Logical OR of the flags of all the packets sent from source to destination IP address	Int	Yes
26	dst2src first seen ms	Timestamp in milliseconds of the first seen packet from destination to source IP address	Int	Yes
27	dst2src last seen ms	Timestamp in milliseconds of the last seen packet from destination to source IP address	Int	Yes
28	dst2src duration ms	Total duration of the destination to source packets in milliseconds	Int	Yes
29	dst2src packets	Total packets sent from destination to source IP address	Int	Yes
30	dst2src bytes	Total bytes sent from destination to source IP address	Int	Yes
31	dst2src min packet size	Minimum packet size sent from destination to source IP address	Int	Yes
32	dst2src max packet size	Maximum packet size sent from destination to source IP address	Int	Yes
33	dst2src mean packet size	Mean of the size of the packets sent from destination to source IP address	Float	Yes
34	dst2src mean packet iat ms	Mean of the inter arrival packet time of all the packets sent from destination to source IP address in milliseconds	Float	Yes
35	dst2src cumulative flags	Logical OR of the flags of all the packets sent from destination to source IP address	Int	Yes
36	classification	Labeling of the dataset (0 or 1)	Int	No
37	category	Category of the classification if present	Str	No

TABLE 6. ANOMAL-E ESTIMATOR MODEL HYPERPARAMETERS

Estimator	Contamination Level	Hyperparameters
PCA	No Contamination	Contamination: 0.02, Number of Components: 0.96, Whiten: False
PCA	3.5% Contamination	Contamination: 0.05, Number of Components: 0.98, Whiten: False
PCA	5.7% Contamination	Contamination: 0.1, Number of Components: 0.98, Whiten: False
CBLOF	No Contamination	Contamination: 0.02, Alpha: 0.9, Beta: 5, Number of Clusters: 36, Use Weights: True
CBLOF	3.5% Contamination	Contamination: 0.05, Alpha: 0.9, Beta: 5, Number of Clusters: 40, Use Weights: True
CBLOF	5.7% Contamination	Contamination: 0.1, Alpha: 0.9, Beta: 5, Number of Clusters: 50, Use Weights: False
HBOS	No Contamination	Contamination: 0.02, Alpha: 0.05, Beta: 5, Number of Bins: 14, Tol: 0.1
HBOS	3.5% Contamination	Contamination: 0.05, Alpha: 0.1, Beta: 5, Number of Bins: 5, Tol: 0.1
HBOS	5.7% Contamination	Contamination: 0.1, Alpha: 0.1, Beta: 5, Number of Bins: 12, Tol: 0.1

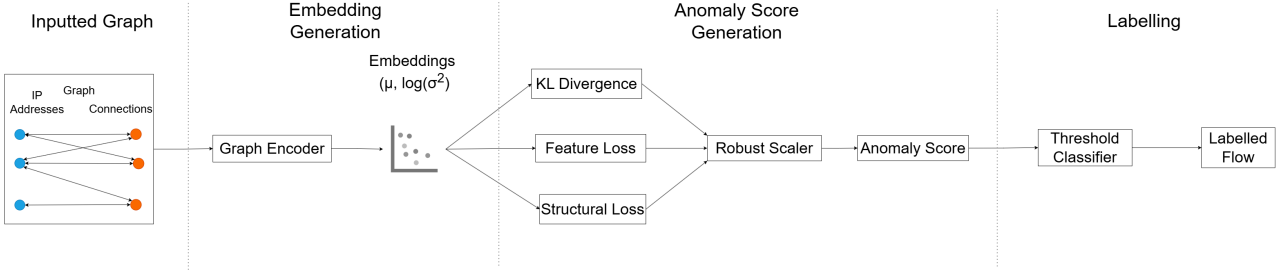


Figure 9. Our Anomaly Score and classification pipeline. The pipeline very closely resembles the training of our model until the first part of the Anomaly Score generation, as once we have the losses, we scale them and combine them to generate the Anomaly Scores of each connection node. Once we have each node score, we pass them through a quantile search to calculate the necessary threshold that will from then on be used to determine if a connection is anomalous or not.

TABLE 7. VGAE MODEL HYPERPARAMETERS

Model Variant	Contamination	Model Hyperparameters
VGAE Regulariser	0%	20% Negative Sampling, Edge Dropping, Node Masking with Annealing, 1 Layer
VGAE Regulariser	3.5%	40% Negative Sampling, Edge Dropping, Node Masking with Annealing, 2 Layers
VGAE Multiple Draw	5.7%	20% Negative Sampling, Edge Dropping, Node Masking with Annealing, 1 Layer, 10 Draws

TABLE 8. VGAE ANOMALY SCORE HYPERPARAMETERS

Contamination	Anomaly Score Hyperparameters
0% Contamination	Alpha: 0.1, Beta: 0.5, Gamma: 0.1, MSE: True, Percentile: 95
3.5% Contamination	Alpha: 1.0, Beta: 0.1, Gamma: 1.0, MSE: False, Percentile: 95
5.7% Contamination	Alpha: 0.5, Beta: 0.1, Gamma: 0.5, MSE: True, Percentile: 95